

X-ray Study on the Incommensurate Phase of α -Bis(*N*-methylsalicylaldiminato)copper(II)* (α -CuNSal)

BY W. ADLHART, H. BLANK AND H. JAGODZINSKI

*Institut für Kristallographie und Mineralogie der Universität München, Theresienstrasse 41, 8 München 2,
Federal Republic of Germany*

(Received 16 December 1981; accepted 22 February 1982)

Abstract

The temperature dependence of satellite reflections and diffuse scattering of α -CuNSal, $\text{Cu}(\text{C}_8\text{H}_8\text{NO})_2$, was studied with X-ray film and counter techniques. At $T_i = 305$ (2) K a continuous and reversible phase transition from a commensurate to an incommensurate orthorhombic structure was observed. At $T_c = 241$ (2) K there occurs a first-order transition from the incommensurate to a commensurate monoclinic structure. In the incommensurate phase an intense diffuse scattering at the satellite reflections was observed, which is explained by phase fluctuations of the static displacement wave.

1. Introduction

Incommensurate structures and associated phase transitions have been the subject of continuous study in recent years (Axe, 1976). Also the α -modification of bis(*N*-methylsalicylaldiminato)copper(II) (α -CuNSal) has an incommensurate structure at room temperature. Its average structure was first refined by Meuthen & von Stackelberg (1960) and by Lingafelter, Simmons, Morosin, Scheringer & Freiburg (1961) in the space group *Ibam*. Yet more recent investigations by Steurer & Adlhart (1981) have shown that the orientation of the thermal ellipsoids violates the mirror symmetry and therefore they conclude that it belongs to the space group *Iba2*.

Meuthen & von Stackelberg (1960) discovered satellite reflections that were later explained by Jagodzinski (1963) and Korekawa (1967) by a transversal sinusoidal displacement of the atoms along *c*. On Weissenberg photographs taken at $T = 338$ K these satellite reflections cannot be observed any more (Adlhart, Peterat & Syal, 1978), only an intense diffuse streak remains. Furthermore, Morosin, Bärtowski, Percy & Samara (1972) observed a phase transition from a high-temperature body-centred orthorhombic to a body-centred monoclinic structure at 210 K.

One aspect of this paper is the study of the behaviour of the satellite reflections in connection with the phase transitions. The results of this study are discussed in § 3. A further subject of recent investigations (Overhauser, 1971; McMillan, 1975, 1976; Axe, 1976) has been the nature of excitations in incommensurate structures. It is assumed that additional to the normal phonon modes there exist further modes corresponding to a fluctuation of the phase and amplitude of the static displacement wave. Very recent experimental results seem to prove these theoretical predictions (Cailleau, Moussa, Zeyen & Bouillot, 1980).

We observe intense diffuse scattering around the satellite reflections and we assume that it is caused by phase fluctuations. In § 4 the diffuse scattering is discussed in connection with calculations of the dynamic structure factor for phase and amplitude fluctuations (Adlhart, 1982).

2. Experimental details

The counter and film measurements were performed with Cu $K\alpha_1$ radiation supplied by a 6 kW rotating anode and a cylindrically bent Ge(111) monochromator. A Weissenberg camera† was modified allowing vacuum conditions and the use of a step motor (ω scan). Normal oscillation and Weissenberg photographs could be taken alternatively. A beryllium tube [length (*l*) = 110 mm, $\varnothing = 57.3$ mm, wall thickness = 0.5 mm] was used as vacuum shield and X-ray window. Because of the vacuum arrangement only the normal-beam technique was possible. The crystal was mounted on a copper bar (*l* = 10 mm, thickness = 1 mm) which was then screwed onto a small copper block. This block was fixed to the goniometer head by a stainless steel tube ($\varnothing = 7$ mm, *l* = 30 mm). Two helical copper wires ($\varnothing = 1$ mm, *l* = 200 mm) maintained the heat transport from the Cu block to a capillary tube connected with a liquid nitrogen container. The copper wires allowed an ω rotation of $\pm 90^\circ$. A cold beryllium radiation shield ($\varnothing = 10$ mm, *l* = 20 mm) was placed

* IUPAC name: α -Bis(*N*-methylsalicylideneiminato)copper(II).

† Huber, D-8211 Rimsting, Federal Republic of Germany.

around the crystal to avoid possible errors in the determination of the crystal temperature. Copper-constantan thermocouples and a three-term proportional integral and derivative controller provided an absolute temperature accuracy of about 2 K and a temperature stability of ± 0.2 K.

The crystals used for the experiments ($0.2 \times 0.4 \times 1$ mm) were needle-shaped along the c direction. An epoxy-resin glue was used to fix them to the copper bar along this direction.

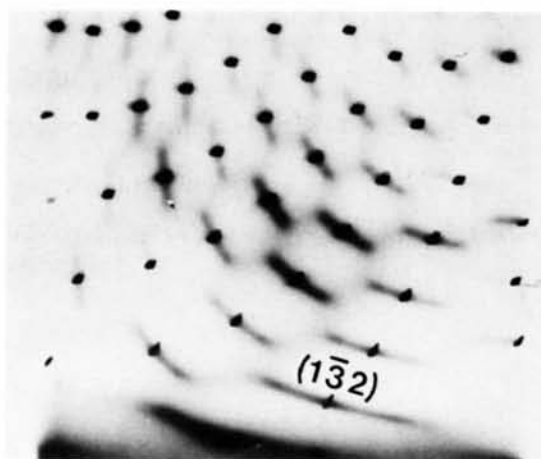
The investigations were performed within the temperature range of 146 to 323 K. The counter measurements focused at the $1\bar{3}2$ reflection and its satellites. Also a satellite of the $1\bar{5}2$ reflection was measured to check the results. For the evaluation of the line positions and integrated intensities Gaussian profiles were fitted to the measured data. The half-width of the line profiles was $0.15\text{--}0.2^\circ$ leading to a relative accuracy in the determination of the wave vector \mathbf{q}_0 of $0.002\mathbf{a}^*$. The absolute accuracy was about $0.004\mathbf{a}^*$.

3. Phase transitions

$hk2$ Weissenberg photographs at 323 K indicate intense diffuse streaks along $\mathbf{a}^*\dagger$ (Fig. 1a). These diffuse streaks cannot be observed for the zero layer (Fig. 2). Therefore we assume that they are caused by displacements of the atoms from their equilibrium positions along c . The diffuse scattering increases with decreasing temperature and at $T_i = 305$ (2) K satellite reflections appear at $\pm \mathbf{q}_0 \simeq 0.3\mathbf{a}^*$ (Fig. 3). This effect is completely reversible. Considering the temperature dependence of the satellite intensities (Fig. 4) we have a continuous and reversible phase transition from the orthorhombic commensurate structure to the orthorhombic incommensurate structure. The satellite reflections can only be observed at layers $l \neq 0$ (see Figs. 2 and 1b); therefore they must be caused by a transverse displacement of the atoms along c . Fig. 5 shows a $[001]$ oscillation photograph illustrating that the main contribution to the diffuse scattering appears in layers where $l = \text{constant}$. Since the satellites and the temperature-dependent diffuse scattering can be explained by displacements of the atoms along c , we conclude that the phase transition originates in the condensation of dynamic atomic movements.

The counter measurements at the $1\bar{3}2$ reflection and its satellites indicate that the intensity of these satellites increases rapidly with decreasing temperature (Fig. 4). From this we infer that the amplitude of the displacement wave increases. For a simple calculation we assume that the atoms perform the same displacements.

\dagger This direction refers to the orthorhombic cell with $a = 9.199$ (2), $b = 24.636$ (5), $c = 6.648$ (2) Å at 300 K and was chosen because in the monoclinic low-temperature cell $\beta \neq 90^\circ$. In earlier publications the standard setting ($a < b < c$) is used.



(a)



(b)



(c)

Fig. 1. Magnified area of $hk2$ normal-beam Weissenberg photographs. (a) $T = 323$ K, orthorhombic commensurate structure; (b) $T = 253$ K, orthorhombic incommensurate structure; (c) $T = 146$ K, monoclinic commensurate structure, twinned crystal.

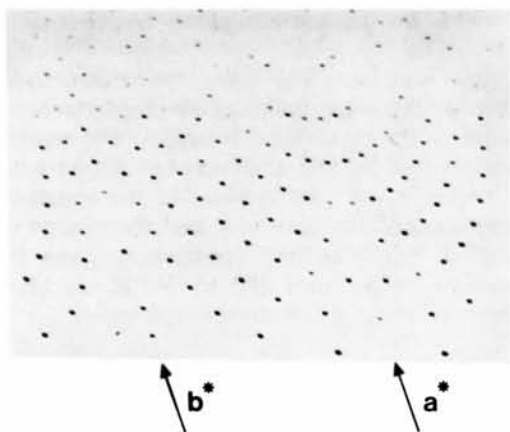


Fig. 2. Section of an $hk0$ Weissenberg photograph at $T = 273$ K.

Neglecting the Q dependence of the Debye–Waller factor as well as the form factor and assuming that phase fluctuations do not influence the intensity of the satellite reflections (see § 4), we get the amplitude A of the displacement wave from

$$\frac{J_1(QA)}{J_0(QA)} = \frac{F_1}{F_0}$$

Here J_0 and J_1 are the Bessel functions of zero and first order. F_0 is the structure factor of the main reflection and F_1 the average structure factor of the two satellites. Fig. 6 shows that at 241 K the amplitude A reaches values of almost 7% of the c lattice constant.

At $T_c = 241$ (2) K we observe a first-order phase transition from the orthorhombic incommensurate to the monoclinic commensurate phase. The transition temperature is approximately the same as reported for α -CuNSal powder [237 (2) K; Adlhart & Syal, 1981].

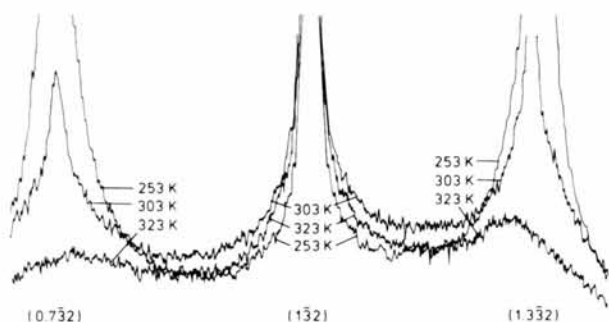


Fig. 3. Photometer curves taken from Weissenberg photographs at various temperatures. The intensity distribution along a^* is shown.

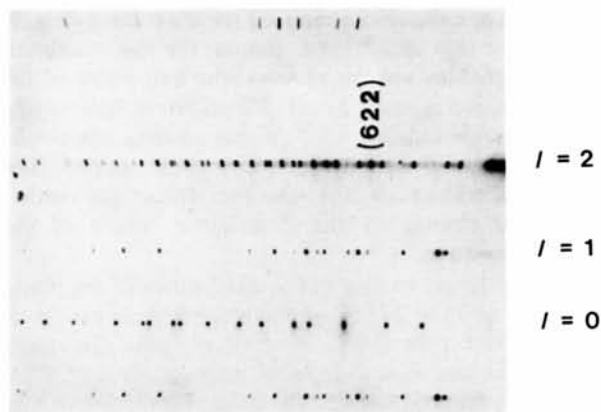


Fig. 5. Section of an $[00l]$ oscillation photograph at $T = 253$ K.

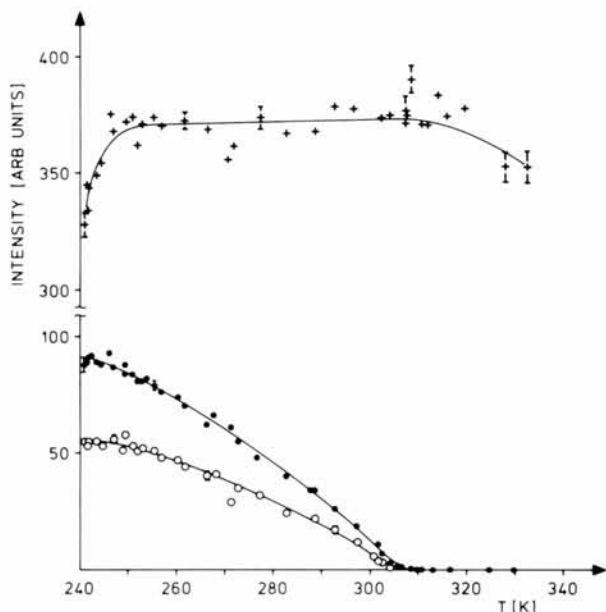


Fig. 4. Integrated intensity of the 132 reflection and its first-order satellites evaluated from the counter measurements. Lorentz, polarization and background corrections were applied. The symbols are: + for the intensity of the main reflection; o for the + q satellite; • for the $-q$ satellite.

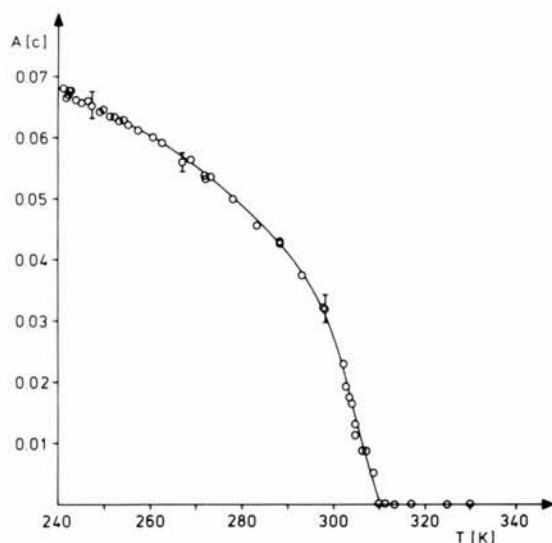


Fig. 6. Amplitude of the static displacement wave as a function of temperature.

At the phase transition the satellite wave vector decreases discontinuously to zero; thus the monoclinic phase has no superstructure (Fig. 1c).

The wave vector of the modulation wave remains almost constant within the temperature range of 303 to 260 K and decreases then to about 3% at the phase transition at 241 K. If the crystal is cooled below the phase transition and then heated again, a wave vector of 0.285 is observed at $T = 241$ K (Fig. 7). At 260 K the same wave vector as before the phase transition is reimposed.

The line profiles of the main reflection $1\bar{3}2$ and its satellites are also broadened (Fig. 8) within the temperature range of 260 to 241 K. Similar to the wave vector, hysteresis effects are also observed for the half-widths. They are measured as a function of the rotation angle ω of the crystal. For temperatures above 260 to 270 K the half-widths are approximately equal for the satellite reflections and the main reflection, but they differ much at lower temperatures. If the results are scaled in units of the reduced wave vector ζ (Fig. 8) we observe that at all temperatures the half-widths of the two satellites are equal, while the half-width of the main reflection is much lower. The different half-widths in the ω scale indicate that the broadening cannot be explained by an increase of the mosaic spread. The equal half-widths of the satellite reflections rather indicate a change of the correlation length of the modulation wave.

In order to get an idea of the mechanism of the phase transition at $T_c = 241$ K we form the first derivative of the modulation wave $\mathbf{u} = \mathbf{A} \sin(\mathbf{q}_0 \mathbf{r})$; using the values $A = 0.066\text{c}$ and $\mathbf{q}_0 = 0.289\mathbf{a}$ we get a gradient of 5° at the nodal points of the sine function. This value can be compared to the deviation of 3° of the angle β from

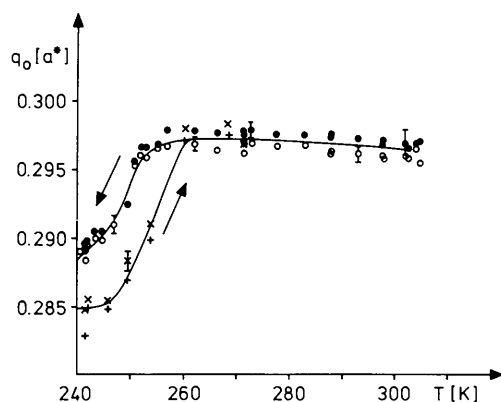


Fig. 7. Temperature dependence of the modulation wave vector measured by counter technique at the first-order satellites of the $1\bar{3}2$ reflection. The symbols are: \circ for the $+\mathbf{q}_0$ wave vector, \bullet for the $-\mathbf{q}_0$ wave vector measured from higher to lower temperatures; $+$ for the $+\mathbf{q}_0$ wave vector, \times for the $-\mathbf{q}_0$ wave vector measured from lower to higher temperatures. Reduced units ζ with $\mathbf{q}_0 = \zeta \mathbf{a}^*$ are given.

90° within the monoclinic phase (Adlhart & Syal, 1981).

In this way we may take the incommensurate structure at the nodal points of the displacement wave as nuclei of the monoclinic structure. The monoclinic twin is formed by the simultaneous decrease of the wave vector \mathbf{q}_0 and the increase of the amplitude \mathbf{A} . The decrease of the \mathbf{q}_0 vector and the change of the correlation length of the modulation wave in the temperature range from 260 to 241 K are taken as precursor effects of this transition mechanism.

4. Phase fluctuations

In the preceding section we have discussed the diffuse scattering along \mathbf{a}^* and its behaviour above the phase transition at T_i . Studying the photometer curve at 253 K (Fig. 3) we observe an intenser diffuse scattering around the satellite reflections than the TDS

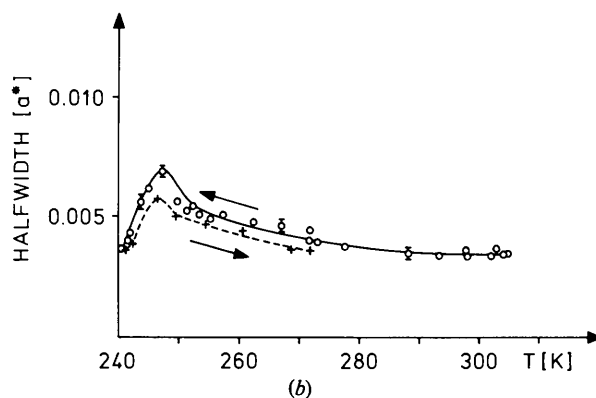
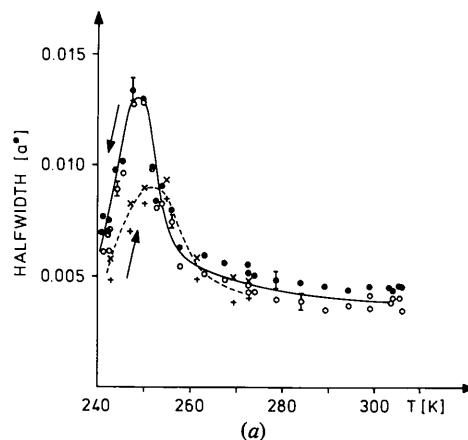


Fig. 8. (a) Half-width of the first-order satellites of the $1\bar{3}2$ reflection in reduced units ζ obtained from ω scans. The symbols have the same meaning as in Fig. 7. The conversion factor from the ω to ζ scale is 0.0217 for the $+\mathbf{q}_0$ and 0.0349 for the $-\mathbf{q}_0$ satellite and 0.0257 for the main reflection. (b) Half-width of the $1\bar{3}2$ reflection. The symbol \circ stands for decreasing measuring temperatures, $+$ indicates rising temperatures.

around the main reflections. This observation is quite striking, since at this temperature the integrated intensity of the main reflection is larger by a factor of five compared with that of the satellites (Fig. 4).

In this section we will try to demonstrate that this observation may be explained by the fact that phase fluctuations of the static displacement wave occur within the incommensurate phase. These phase fluctuations were introduced by Overhauser (1971) as 'phasons', standing for vibrational excitations of the phase of the static modulation wave. Even though these phasons seem to have been observed (Cailleau *et al.*, 1980) we may not give direct evidence of the dynamic character of possible excitations as far as our X-ray experiments are concerned.

We would like to discuss our experiments with the help of recent dynamic structure-factor calculations (Adlhart, 1982). We anticipate that the main part of the diffuse scattering around the satellites is caused by phasons, since their dispersion relation approaches zero at the site of the satellite reflections. Amplitudons are neglected because their frequency spectrum has a gap at the site of the satellite reflections (McMillan, 1975).

The equations relevant for our discussion are (15), (16) and (19) from Adlhart (1982), describing the elastic structure factor

$$F_m(\mathbf{Q}) = \delta(\mathbf{Q} + m\mathbf{q}_0 - \mathbf{G}) J_m(\mathbf{QA}) \times \sum_{\kappa} f_{\kappa} \exp(-W_{\kappa}) \exp(i\mathbf{G}\mathbf{r}_{\kappa}), \quad (1)$$

the phonon structure factor

$$F_m^U(\mathbf{Q}) = \delta(\mathbf{Q} + \mathbf{q} + m\mathbf{q}_0 - \mathbf{G}) J_m(\mathbf{QA}) \left(\frac{\mathbf{QU}_q}{2} \right) \times \sum_{\kappa} f_{\kappa} \exp(-W_{\kappa}) \exp(i\mathbf{G}\mathbf{r}_{\kappa}), \quad (2)$$

and the phason structure factor

$$F_m^{\Phi}(\mathbf{Q}) = \delta(\mathbf{Q} + \mathbf{q} + m\mathbf{q}_0 - \mathbf{G}) m J_m(\mathbf{QA}) \frac{\Phi_q}{2} \times \sum_{\kappa} f_{\kappa} \exp(-W_{\kappa}) \exp(i\mathbf{G}\mathbf{r}_{\kappa}). \quad (3)$$

$\{\mathbf{G}\}$ is the total set of reciprocal-lattice vectors, W_{κ} the usual Debye-Waller factor, and \mathbf{U}_q and Φ_q are the amplitudes of the phonon and phason modes, respectively. For the sake of simplicity equal amplitudes and phases were assumed for all atoms of the unit cell for the modulation wave and the modes.

Equation (2) shows that acoustic phonons can also be observed around satellite reflections. By comparing this intensity with the TDS around main reflections we get with (1) and (2)

$$\frac{F_1^U(\mathbf{Q})}{F_0^U(\mathbf{Q})} \simeq \frac{F_1(\mathbf{Q})}{F_0(\mathbf{Q})}.$$

The \mathbf{Q} dependences of f_{κ} and W_{κ} are neglected.

Since the intensity of the satellite reflections amounts only to about $\frac{1}{5}$ of that of one of the main reflections, the intense diffuse scattering around the satellites cannot stem from the acoustic modes.

Following (3) no scattering of phasons is possible around main reflections, because in this case $m = 0$. Equation (3) becomes more complicated if we introduce the influence of phase and amplitude fluctuations (Adlhart, 1982) to the structure-factor calculation. In this case phasons contribute to the scattering around main reflections. However, for small values of \mathbf{QA} ($\mathbf{QA} \simeq 0.75$ for the $1\bar{3}2$ reflection at $T = 253$ K) their contribution will not be observable.

On the other hand, phasons may produce strong diffuse scattering around the satellite reflections [equation (3), $m = 1$] and therefore, in accordance with our observations, the diffuse scattering around satellite reflections may be intenser than around the main reflection.

5. Anharmonicities

Satellites of second order can easily be discerned on the $hk2$ Weissenberg photograph (Fig. 1b). Either they may represent so-called 'diffraction harmonics', *i.e.* second-order satellites at $\mathbf{Q} = \mathbf{G} \pm 2\mathbf{q}_0$ which are caused by a perfect sinusoidal modulation wave, or they may stem from the first anharmonic contribution of the modulation wave with the wave vector $2\mathbf{q}_0$.

In the first case the structure factor $F_2(\mathbf{Q})$ for the second-order satellite is, with respect to the approximation given in § 4,

$$F_2(\mathbf{Q}) = \frac{J_2(\mathbf{QA})}{J_0(\mathbf{QA})} F_0(\mathbf{Q}).$$

In order to investigate the influence of the anharmonicities we calculated the amplitude A by comparing five $hk2$ reflections and their second-order satellites and got $A_2 = 0.29 \pm 0.05 \text{ \AA}$ at 253 K. The same procedure for 11 $hk2$ reflections and their first-order satellites yields $A_1 = 0.38 \pm 0.003 \text{ \AA}$, whereas the counter measurements (Fig. 4) give an amplitude of $A_1 = 0.35 \pm 0.01 \text{ \AA}$. This comparison indicates that the second-order satellites have the character of diffraction harmonics. However, anharmonic contributions may not be excluded completely, because phase shifts between the modulating functions with wave vectors \mathbf{q}_0 and $2\mathbf{q}_0$ may lower the intensity of the second-order satellite. Furthermore, phase fluctuations tend to attenuate second-order satellites more than first-order satellites; this may possibly explain the low value of A_2 .

6. Conclusion

Our X-ray investigations on α -CuNSal have shown a reversible and continuous structural phase transition from a commensurate to an incommensurate orthorhombic phase at $T_i = 303$ K and a reversible first-order phase transition into a monoclinic commensurate phase at 241 K. There also exists an intense temperature-dependent diffuse scattering along \mathbf{a}^* and we assume that it is caused by dynamic atomic movements associated with the phase transition at T_i . Within the incommensurate phase we observe a pronounced diffuse scattering around the satellite reflections which is explained by phase fluctuations of the modulation wave. The results are discussed within the frame of a simple model assuming equal amplitudes of the modulation wave for all atoms of the chelate molecule.

At the moment refinements of the structures within the three phases are performed and we hope that these investigations will supply important information on the dynamic processes at the phase transition.

This project was supported by the Deutsche Forschungsgemeinschaft, Projekt Ja 15/32, Ja 15/34.

Acta Cryst. (1982). A38, 510–512

The Polarization Factor for a Repeatedly Reflected X-ray Beam: Special Cases

BY M. G. VINCENT

Abteilung Strukturbiologie, Biozentrum, Klingelbergstrasse 70, CH-4056 Basel, Switzerland

(Received 28 January 1982; accepted 23 February 1982)

Abstract

A method for determining the polarization factor for a repeatedly reflected X-ray beam is described. It is shown that, provided the relative orientations of the pre-specimen reflectors are restricted to special geometries (the usual cases), the appropriate expression for an unpolarized beam reflected m times can be simply derived. The treatment is extended to a plane-polarized beam, resulting in an expression dependent on polarization effects from the specimen alone and hence independent of the state of perfection of crystal monochromators. The latter expression may have some relevance to experiments performed with synchrotron radiation.

Many of the techniques used today for measuring X-ray diffraction data have as an integral part of their

References

- ADLHART, W. (1982). *Acta Cryst.* A38, 498–504.
 ADLHART, W., PETERAT, M. & SYAL, V. K. (1978). *Acta Cryst.* A34, S 125.
 ADLHART, W. & SYAL, V. K. (1981). *Z. Kristallogr.* 154, 227–233.
 AXE, J. D. (1976). ORNL Report CONF-760 601-P1, pp. 353–378. Oak Ridge National Laboratory, Tennessee.
 CAILLEAU, H., MOUSSA, F., ZEYEN, C. M. E. & BOUILLOT, J. (1980). *Solid State Commun.* 33, 407–411.
 JAGODZINSKI, H. (1963). *Crystallography and Crystal Perfection*, edited by G. N. RAMACHANDRAN, pp. 177–188. London, New York: Academic Press.
 KOREKAWA, M. (1967). *Theorie der Satellitenreflexe*. Habilitation, Univ. München.
 LINGAFELTER, E. C., SIMMONS, G. L., MOROSIN, B., SCHERINGER, C. & FREIBURG, C. (1961). *Acta Cryst.* 14, 1222–1225.
 MCMILLAN, W. L. (1975). *Phys. Rev. B*, 12, 1187–1196.
 MCMILLAN, W. L. (1976). *Phys. Rev. B*, 14, 1496–1502.
 MEUTHEN, B. & VON STACKELBERG, M. (1960). *Z. Anorg. Chem.* 305, 279–285.
 MOROSIN, B., BARTOWSKI, R. R., PEERCY, P. S. & SAMARA, G. A. (1972). *Acta Cryst.* A28, S 177.
 OVERHAUSER, A. W. (1971). *Phys. Rev. B*, 3, 3173–3182.
 STEURER, W. & ADLHART, W. (1981). *Acta Cryst.* A37, C232.

instrumentation a system of pre-reflectors, reflecting the beam before diffraction by the specimen takes place. Such systems may include one or more crystal monochromators and/or focusing mirrors, usually serving either to select a particular wavelength of radiation or to produce a convergent beam of X-rays. The common feature of most – if not all – these arrangements is the relative orientations of the pre-specimen reflectors with respect to one another and, in some cases, to the specimen itself. These geometries are restricted to two types: those in which the diffraction plane (the plane containing the incident and reflected beams) of the i th reflector is parallel to the diffraction plane of the first reflector ($\rho = 0^\circ$ geometry), and those in which the diffraction planes of the first and i th reflectors are perpendicular to each other ($\rho = 90^\circ$ geometry).

A general formula for the polarization factor for a system of one monochromator plus specimen has been